JBUON 2021; 26(4): 1279-1291
ISSN: 1107-0625, online ISSN: 2241-6293 • www.jbuon.com
Email: editorial_office@jbuon.com

ORIGINAL ARTICLE

FTO-stabilized lncRNA HOXC13-AS epigenetically upregulated FZD6 and activated Wnt/β-catenin signaling to drive cervical cancer proliferation, invasion, and EMT

Tongfei Wang[1], Weina Li[2], Biaofei Ye[1], Shuangyan Zhang[1], Xin Lei[1], Da Zhang[3]

[1]Department of Oncology, Xi'an No.3 Hospital, the Affiliated Hospital of Northwest University, Xi'an, China. [2]Biotechnology Center, School of Pharmacy, Fourth Military Medical University, Xi'an, China. [3]Department of Oncological Surgery, Xi'an No.3 Hospital, the Affiliated Hospital of Northwest University, Xi'an, China.

Summary

Purpose: *Cervical cancer (CC) is the third most prevalent malignancy in women. Frizzled class receptor 6 (FZD6) is demonstrated to either activate or repress the activity of Wnt/β-catenin pathway, a crucial signaling involved in cancer development. However, the role of FZD6 in CC is unknown. The present study explored the function of FZD6 and its mechanism in CC.*

Methods: *The levels of FZD6, HOXC13-AS were detected in CC specimens and CC cell lines via qRT-PCR. Cell proliferation and invasion was explored via CCK-8 assay, colony formation assay and transwell assay. Luciferase reporter analysis, FISH, subcellular fractionation, chromatin immunoprecipitation and RNA immunoprecipitation were performed for investigating the molecular mechanism.*

Results: *FZD6 was up-regulated in CC. FZD6 silence retarded proliferation, invasion, and epithelial-to-mesenchymal transition (EMT), and inactivated Wnt/β-catenin. HOXC13 antisense RNA (HOXC13-AS) was up-regulated in CC and positively correlated with FZD6. Mechanistically, HOCX13-AS1 augmented FZD through cAMP-response element binding protein-binding protein (CBP)-modulated histone H3 on lysine 27 acetylation (H3K27ac). Additionally, fat mass and obesity-associated protein (FTO) reduced N6-methyladenosine (m6A) and stabilized HOXC13-AS in CC.*

Conclusions: *In conclusion, this study firstly showed that FTO-stabilized HOXC13-AS epigenetically up-regulated FZD6 and activated Wnt/β-catenin signaling to drive CC proliferation, invasion, and EMT, suggesting HOXC13-AS as a potential target for CC treatment.*

Key words: *cervical cancer, FZD6, HOXC13-AS, H3K27ac, m6A*

Introduction

Cervical cancer (CC) is recognized as the third most prevalent malignancy in women globally, and its mortality is high [1]. Although past decades witnessed advancement in the treatment approaches and diagnostic techniques for CC, the 5-year overall prognosis in CC patients is yet to be further improved [2,3]. Hence, better understanding of CC development is urgently required to improve the therapies in CC patients.

Frizzled class receptors (FZD) are receptors of the Wnt molecules, and regulate the activity of Wnt/β-catenin signaling through Wnt binding [4]. FZD receptors are dysregulated and deeply involved in tumorigenesis, such as in colorectal cancer and breast cancer [5,6]. FZD6, a member of FZD family, is reported to present up-regulation in multiple cancers [7-11]. Although some studies delineated that FZD6 repressed Wnt/β-catenin

Corresponding author: Da Zhang, MD. Department of Oncological Surgery, Xi'an No.3 Hospital, the Affiliated Hospital of Northwest University, 10 East Section of Fengcheng Third Rd, Weiyang District, Xi'an, Shaanxi 710018, China
Tel: +86 018629091015; Email: Dazhangsurgery@163.com
Received: 29/04/2021; Accepted: 22/05/2021

[12], other studies argued that FZD6 can activate Wnt/β-catenin. For example, FZD6 interacted with Wnt4 to activate Wnt/β-catenin/LEF/TCF signaling cascades [13]. Also, Chen et al showed that lncFZD6 activated FZD6 transcription to promote nuclear translocation of β-catenin and activate Wnt signaling, and suggested that the function of FZD6 may vary depending on cell types [14]. However, the implication of FZD6 in CC is elusive.

Long non-coding RNAs (lncRNAs) are unceasingly reported to be closely related to carcinogenesis of various cancer types [15-17]. As a group of RNA transcripts (≥200 bp) unable to be translated into proteins [18], lncRNAs regulate functional genes in cancer cells epigenetically [19], transcriptionally [20], or post-transcriptionally [21]. Numerous lncRNAs are identified to participate in cancer progression, including CC [15,19]. HOXC13-AS was identified as a carcinogene in breast cancer and nasopharyngeal carcinoma [22,23]. Nevertheless, association between HOXC13-AS and CC has never been established.

N6-methyladenosine (m6A) is a common modification of mRNA in mammalians [24,25]. The m6A modification influences mRNA processing in multiple aspects, such as RNA degradation, alternative splicing, as well as translation [26,27]. Recent studies showed that m6A modification is responsible for the dysregulation of lncRNAs [28,29]. Fat mass and obesity-associated protein (FTO), a m6A demethylase, is reported to be oncogenic in several cancers such as pancreatic [30], breast [31], and endometrial cancer [32]. Notably, a study showed that FTO was up-regulated in CC and stabilized the mRNA of β-catenin through reducing its m6A level [33]. However, whether FTO-mediated m6A influenced HOXC13-AS expression remains unknown. Hence, this study aimed to explore the role of FZD6 in CC.

Methods

Clinical samples

Written informed consent form was signed by all patients, and the ethical approval was acquired from the Ethics Committee of Xi'an No.3 Hospital (2013CN-SXX-A3H-no.MC100542) (the Affiliated Hospital of Northwest University). 52 CC and adjacent non-tumor tissue samples were collected from patients who did not receive radiotherapy and chemotherapy before resection between 2013 and 2018. All samples were instantly preserved in liquid nitrogen at -80°C.

Cell lines

CC cell lines (C33A, C4-1, HeLa, SiHa) and normal cervical cell line (Crl-2614), from Chinese Type Culture Collection (Shanghai, China), were grown in Dulbecco's Modified Eagle's Medium (DMEM) with 10% fetal bovine serum (FBS) (Thermo Fisher Scientific, Waltham, MA, USA) contusing antibiotics at 37°C in 5% CO_2.

Extraction of total RNA and real-time quantitative polymerase chain reaction (qRT-PCR)

Total RNA was extracted from SiHa and HeLa cells by TRIzol (Invitrogen, Carlsbad, CA, USA) for synthesizing complementary deoxyribose nucleic acid (cDNA) with Revert Aid First Strand cDNA Synthesis Kit (Thermo Fisher, Waltham, MA, USA). qRT-PCR was performed with SYBR Green Master Mix (TaKaRa, Tokyo, Japan), followed by $2^{-\Delta\Delta Cq}$ method for quantification. The cycling conditions were: pre-denaturation at 95°C for 10 min, 40 cycles of denaturation at 95°C for 15 s, annealing at the appropriate temperature for 1 min and extension at 72°C for 30 s. The specific primers were listed as follows: Forward Primer for FZD6, 5'-ATGGCCTACAACATGACGTTT-3', Reverse Primer for FZD6, 5'-GTTTACGACAAGGTGGAACCA-3'; Forward Primer for FTO, 5'-ACTTGGCTCCCTTATCTGACC-3', Reverse Primer for FTO, 5'-TGTGCAGTGTGAGAAAGGCTT-3'; Forward Primer for CBP, 5'-TTCCTGTGCTCTAGTTGTGACA-3', Reverse Primer for CBP, 5'-CACGTTCATCAGGTTCTCATGG-3'; Forward Primer for HOXC13-AS, 5'-GCCGTCTATACGGACATCCC-3', Reverse Primer for HOXC13-AS, 5'-GGTAGGCGCAAGGCTTCTG-3'.

Cell transfection

Cells in 6-well plates were separately transfected with various specific shRNAs and pcDNA3.1 vectors for 48 h using Lipofectamine2000 (Invitrogen, Carlsbad, CA, USA). The duplicate shRNAs for FZD6, HOXC13-AS, CBP, FTO, and pcDNA3.1/CBP, pcDNA3.1/FZD6, as well as controls (sh-NC and empty vector) were all produced by GeneChem (Shanghai, China). The 5'-3' sequences of specific shRNAs were listed as follows: sh-FZD6#1, 5'-GAGAGCGAGGGGCACGCCGAGAGCTCCG-3', sh-FZD6#2, 5'-ACCCTGACCCGTCCCCGGCCCGCCCACG-3', sh-NC, 5'-CGGTGGGTTAGACGGGGACGGGAAGGGA-3'; sh-HOXC13-AS#1, 5'-TCCGCTTGAGGAACCGGGATCTCCTGTC-3', sh-HOXC13-AS#2, 5'-CACCTACGTCCTCGTCGCTTCAGCAGTA-3', sh-NC, 5'-AAATCCGCCGGCTCCCGCTCTCCACCTC-3'; sh-CBP#1, 5'-ACATTCCTTTTGCATCGCTTTTAACTCC-3', sh-CBP#2, 5'-GAATCGTAGTGTTTCGCCTGTCCTTTCT-3', sh-NC, 5'-ATTAACTTTTCATTCCCGCATTATTAAT-3'; sh-FTO#1, 5'-ACACTCGTTCCTAGTCCCTTGGCCTTCC-3', sh-FTO#2, 5'-CGTAGATAAGGAACCAATTTAAACAGCG-3', sh-NC, 5'-ATAACAGCCCAGCTTCACAGATGAAGAA-3'.

Cell proliferation assay

For CCK-8 assay, 10 μL of cell counting kit-8 (CCK-8) reagent (Dojindo, Kumamoto, Japan) was added and CC cells were cultured in 96-well plates (1×10^3 cells/well) for 2 h. The absorbance was monitored at 450 nm by microplate reader.

For colony formation assay, CC cells in 6-well plates were incubated for 14 days, and subjected to methanol fixation and crystal violet staining. Colonies (>50 cells) were defined as surviving colonies.

Transwell invasion assay

CC cells were planted to the upper chamber of Matrigel-coated transwell insert (Corning, Corning, NY, USA), while complete medium was added to the lower chamber. 48 h later, invasive CC cells were fixed and stained with crystal violet, following counting under the microscope.

Luciferase reporter analysis

To assay the Wnt/β-catenin signaling pathway activity, TOP Flash and FOP Flash reporter vectors covering the wild-type or mutant TCF binding sites were available from Addgene (Cambridge, MA, USA). SiHa and HeLa cells were placed in 24-well plates for co-transfecting for 48 h with the TOP/FOP Flash and indicated transfection plasmids by using the Lipofectamine2000. The transfection plasmids, including sh-FZD6#1/2 or sh-NC group, sh-HOXC13-AS#1/2 or group, and sh-NC, sh-HOXC13-AS#1, sh-HOXC13-AS#1 + pcDNA3.1 or sh-HOXC13-AS#1 + pcDNA3.1/FZD6 group, were used for assessing Wnt/β-catenin activity. Besides, CC cells were co-transfected with pGL3 vector containing FZD6 promoter, the pRL-TK-Renilla plasmid and sh-HOXC13-AS and sh-NC. Luciferase activity was analyzed after transfection by Luciferase reporter assay system (Promega, Madison, WI, USA).

Western blotting

Cellular protein samples in radioimmunoprecipitation assay (RIPA) buffer were electrophoresed on 10% sodium dodecyl sulphate-polyacrylamide gel electrophoresis (SDS-PAGE) and then transferred to polyvinylidene fluoride (PVDF) membranes. The primary antibodies including rabbit polyclonal anti-human β-catenin antibody (ab2365), rabbit polyclonal anti-human H3 antibody (ab1791), mouse monoclonal anti-human GAPDH antibody (ab9484), rabbit monoclonal anti-human c-Myc antibody (ab32072), mouse monoclonal anti-human E-cad antibody (ab1416), rabbit polyclonal anti-human N-cad antibody (ab18203), rabbit polyclonal anti-human MMP2 antibody (ab97779), rabbit polyclonal anti-human MMP7 antibody (ab5706), rabbit polyclonal anti-human FZD6 antibody (ab98933), rabbit polyclonal anti-human CBP (ab42389) antibody, and secondary antibody, were acquired from Abacm (Cambridge, MA, USA). All signals were assayed by ECL detection system (Amersham Pharmacia, Piscataway, New Jersey, USA).

FISH

RNA FISH probe for HOXC13-AS was synthesized by RiboBio (Guangzhou, China). Nuclei were counterstained with 4',6-diamidino-2-phenylindole (DAPI) (RiboBio, Guangzhou, China) then analyzed by confocal microscope.

Subcellular fractionation

Using Cytoplasmic-Nuclear RNA Purification Kit (Norgen, Belmont, CA, USA), cytoplasm and nucleus of CC cells were isolated and finally detected by qRT-PCR. GAPDH served as the cell cytoplasm indicator, while U6 served as the cell nucleus indicator.

Chromatin immunoprecipitation (ChIP)

Cell samples were first crosslinked for 10 min in 4% (v/v) formaldehyde at room temperature. Chromatin DNA was then re-suspended in the lysis buffer and sonicated for immunoprecipitation with specific antibodies on the magnetic beads. IgG antibody acted as negative control. After washing and de-crosslinking, quantification of precipitates was conducted by qRT-PCR.

RNA immunoprecipitation (RIP)

Using Magna RIP Kit (Millipore, Billerica, MA, USA), RIP assay was performed. 1×10^7 cultured CC cells were rinsed in PBS and lysed in the RIP lysis buffer adding the protease inhibitor and RNase inhibitor. 100 μL of cell lysates were cultured with the RIP buffer adding the magnetic beads bound with anti-m6A (ab208577), anti-CBP (ab42389), anti-BRG1 (ab110641), positive control anti-SNRNP70 (03-103; Millipore, Billerica, MA, USA) or negative control anti-IgG (ab205719). After digestion, the precipitated RNAs were assessed by qRT-PCR.

Statistics

Data were analyzed by SPSS 18.0 (Chicago, Illinois, USA) as mean ± SD (standard deviation) from independent triplicates. Gene correlation was examined by Pearson's method. Student's t-test and analysis of variance (ANOVA) were used for group comparison, with threshold of $p<0.05$.

Results

Expression and biological function of FZD6 in CC

First, TCGA datasets revealed that FZD6 level was elevated in cervical squamous cell carcinoma and endocervical adenocarcinoma (CESC) samples (Figure 1A). Accordingly, qRT-PCR data verified the up-regulation of FZD6 in CC specimens (Figure 1B). Besides, CC cell lines presented higher FZD6 level than normal cells (Figure 1C). Next, we interrogated the biological impacts of FZD6 in CC cells. According to qRT-PCR data, FZD6 was overtly silenced in SiHa and HeLa cells which expressed high FZD6 level (Figure 1D). Proliferation and invasion in CC cells were abrogated upon FZD6 silence (Figures 1E-1G). The migration declined due to decrease of FZD6 as well (Supplementary Figure 1A). Since FZD6 is documented to activate Wnt/β-catenin to exert oncogenic effects [14], we examined its influence on Wnt/β-catenin in CC cells. The activity of Wnt/β-catenin declined upon FZD6 knockdown (Figure 1H). The nuclear level of β-catenin dropped under FDZ6 silence with the accumulation of β-catenin in cytoplasm (Figure 1I & Supplementary Figure 1B). Effectors downstream Wnt/β-catenin including c-Myc, N-cadherin (N-cad), MMP2, and MMP7 decreased, whereas E-cadherin (E-cad) increased under FZD6 silence (Figure

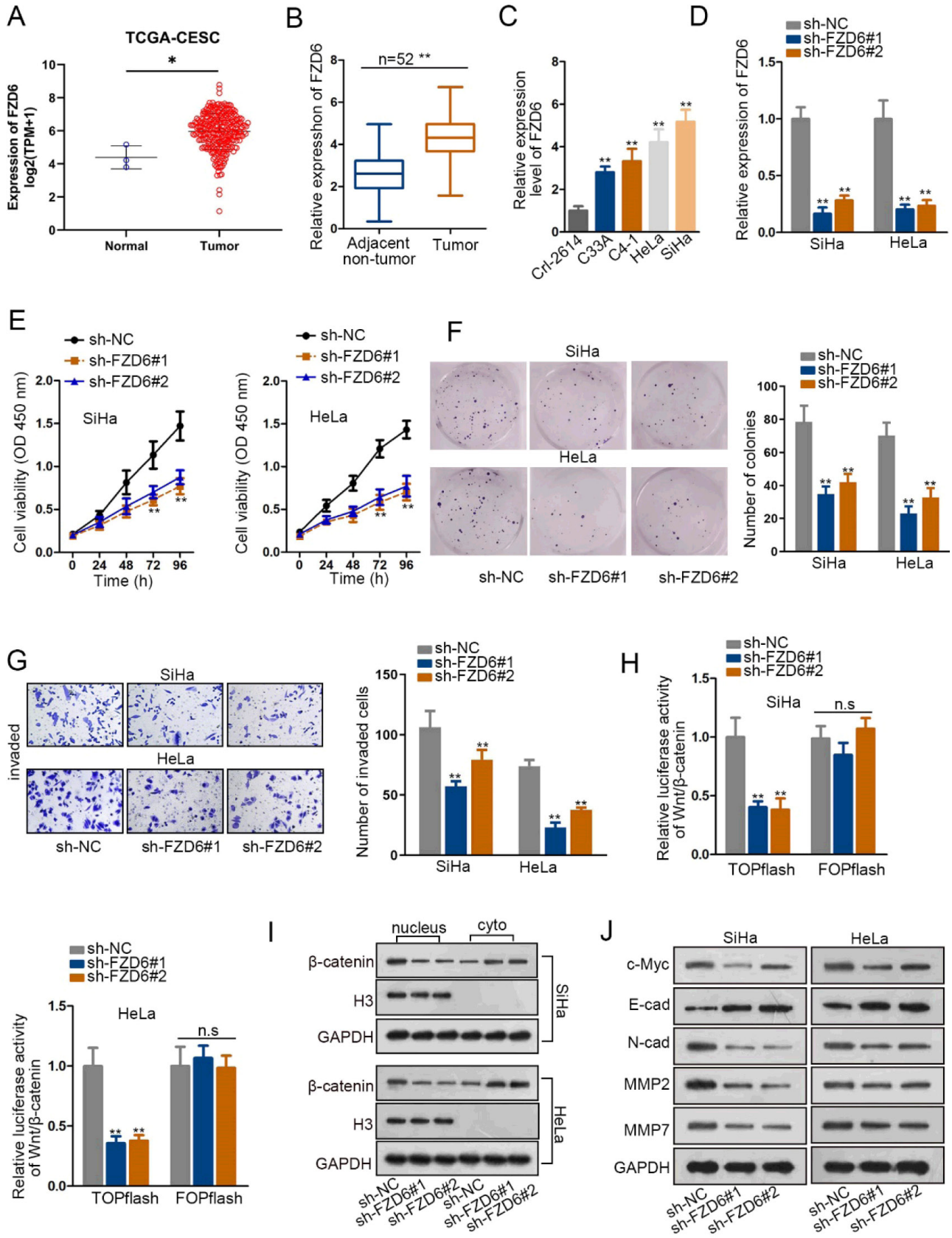

Figure 1. Expression and biological function of FZD6 in CC. **A:** FZD6 level in CESC tissues of TCGA datasets. **B-C:** RT-qPCR analyses FZD6 level in CC tissues and CC cell lines. **D:** RT-qPCR data of the silence of FZD6 in SiHa and HeLa cells. **E-G:** Proliferation and invasion of CC cells were tested by CCK-8, colony formation and Transwell assays. **H:** TOP-flash analysis of Wnt/β-catenin activity under FDZ6 silence. **I:** Western blot of nuclear and cytoplasmic β-catenin in CC cells upon FZD6 knockdown. **J:** Western blotting of effectors downstream Wnt/β-catenin including c-Myc, E-cad, N-cad, MMP2, and MMP7. *p<0.05; **p<0.01.

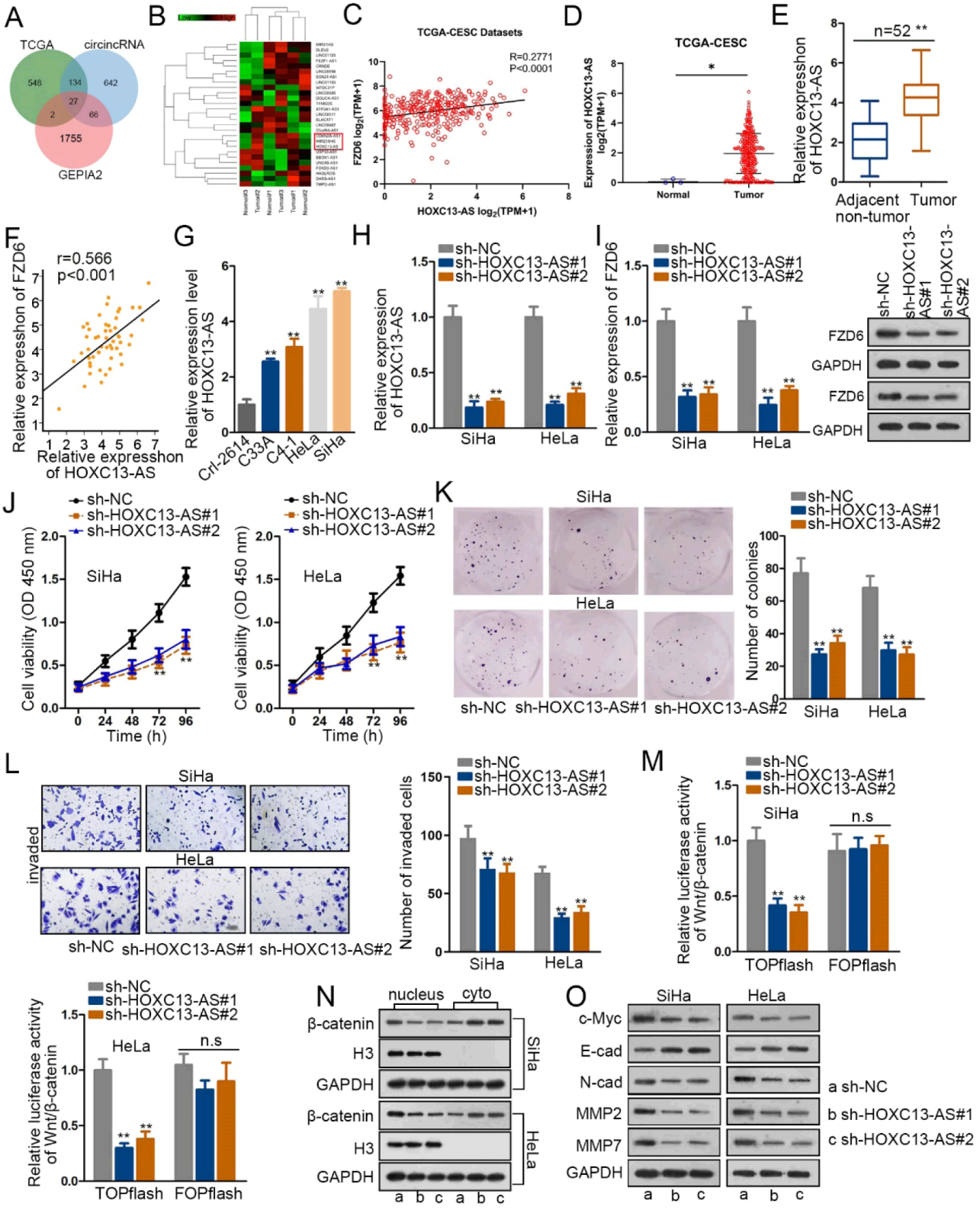

Figure 2. HOXC13-AS up-regulated FZD6 and facilitated proliferation, invasion, and Wnt/β-catenin activity in CC. **A-B:** 27 lncRNAs up-regulated in CESC tissues from bioinformatics tools were subjected to RT-qPCR analysis in CC tissues. **C-F:** HOXC13-AS presented up-regulation and positive correlated with FZD6 in CESC samples of TCGA and in CC tissues. **G:** RT-qPCR data of HOXC13-AS Up-regulation in CC cell lines. **H:** RT-qPCR data of HOXC13-AS knockdown in HeLa and SiHa cells. **I:** FZD6 mRNA and protein levels under HOXC13-AS depletion. **J-L:** Growth curve and representative pictures and quantification of colony formation and invasion of CC cells upon HOXC13-AS depletion were displayed. **M-N:** TOP-flash activity of Wnt/β-catenin and the nuclear translocation of β-catenin. "a b c" stand for sh-NC, sh-HOXC13-AS#1 and sh-HOXC13-AS#2. **O:** Western blots of c-Myc, E-cad, N-cad, MMP2, and MMP7 upon HOXC13-AS silence. *p<0.05; **p<0.01. Here "a b c" stands for sh-NC, sh-HOXC13-AS#1 and sh-HOXC13-AS#2.

1J & Supplementary Figure 1C & Supplementary Figure 1D). Together, FZD6 was up-regulated in CC and silencing FZD6 reduced proliferation, invasion, and Wnt/β-catenin activity *in vitro*.

HOXC13-AS up-regulated FZD6 and facilitated proliferation, invasion, and Wnt/β-catenin activity in CC

Thereafter, we interrogated the mechanism underlying FZD6 up-regulation in CC. LncRNAs are widely known as pivotal modulators of gene expression in cancer [19-21]. We analyzed the TCGA datasets to identify the significantly up-regulated lncRNAs in CESC samples ($p<0.05$, log2FC>1) and compared the data in two bioinformatics websites GEPIA2 (http://gepia.cancer-pku.cn/index.html) and circlncRNAnet (http://120.126.1.61/circlnc/circlncRNAnet/lncRNA_TCGA/index.php). Consequently, 27 lncRNAs up-regulated in CESC were sorted out (Figure 2A). Through qRT-PCR, we observed that among 27 candidates, CDKN2B-AS1, HOXC13-AS, and MIR205HG were the top-3 up-regulated lncRNAs in CC tissues (Figure 2B). However, only HOXC13-AS presented positive relation with FZD6 in CESC samples referring to TCGA data (Figure 2C). Up-regulation of HOXC13-AS in TCGA data was presented in Figure 2D, and confirmed in CC tissues via RT-qPCR (Figure 2E). Later, we validated the positive correlation between HOXC13-AS and FZD6 in CC tissues (Figure 2F). High HOXC13-AS level in CC cell lines was observed (Figure 2G). qRT-PCR experiment verified HOXC13-AS knockdown in HeLa and SiHa cells (Figure 2H). We monitored that FZD6 mRNA and protein levels dropped with HOXC13-AS knockdown (Figure 2I). Functionally, HOXC13-AS depletion impeded proliferation and invasion along with migration in CC cells (Figure 2J-2L & Supplementary Figure 1E). Moreover, ablation of HOXC13-AS inactivated Wnt/β-catenin and prevented the nuclear translocation of β-catenin (Figure 2M-2N & Supplementary Figure 1F). Levels of c-Myc, N-cad, MMP2 and MMP7 decreased, whereas E-cad increased upon HOXC13-AS silence (Figure 2O & Supplementary Figure 1G).

HOXC13-AS induced H3K27ac on FZD6 promoter through interacting with CBP

Subsequently, we searched how HOXC13-AS up-regulated FZD6 in CC cells. FISH and subcellular fractionation depicted the localization of HOXC13-AS mainly in nucleus (Figure 3A). Hence, we tried to assess whether HOXC13-AS influenced FZD6 transcription. Expectedly, HOXC13-AS depletion reduced luciferase activity of FZD6 promoter (Figure 3B). UCSC genome browser (http://genome.ucsc.edu/) showed H3K27ac enrichment at CpG island of FZD6 promoter (Figure 3C). So we deduced that HOXC13-AS regulated FZD6 epigenetically through H3K27ac. ChIP analysis showed that silencing HOXC13-AS reduced the abundance of FZD6 promoter in H3K27ac precipitates (Figure 3D). It has been reported that lncFZD6 interacted with BRG1 to regulate H3K27ac at FZD6 promoter [14], so we wondered whether HOXC13-AS regulated FZD6 through this way. However, RIP assay showed that HOXC13-AS was not enriched in the binding complex of BRG1 (Figure 3E). Besides BRG1, CBP is a well-known histone acetyltransferase regulating H3K27ac [34]. Interestingly, RIP showed enrichment of HOXC13-AS in CBP precipitates (Figure 3E). Hence, we deduced that HOXC13-AS interacted with CBP to induce H3K27ac of FZD6. We used qRT-PCR analysis to find CBP expression was diminished due to sh-HOXC13-AS#1/2 transfected into SiHa and HeLa cells (Supplementary Figure 1H). We confirmed that CBP knockdown significantly reduced the mRNA and protein of CBP and FZD6 (Figure 3F). ChIP analysis revealed that pcDNA3.1/CBP stabilized the repressive effect of sh-HOXC13-AS#1 on the enrichment of H3K27ac and CBP on FZD6 promoter (Figure 3G). FZD6 expression was reduced by sh-HOXC13-AS#1 and was restored by pcDNA3.1/CBP (Figure 3H).

FTO-stabilized HOXC13-AS facilitated CC cell proliferation, invasion and Wnt/β-catenin activity through FZD6

Furthermore, we investigated how HOXC13-AS was up-regulated in CC. m6A modification is reported to influence lncRNA expression [28,29]. The m6A RIP delineated that m6A level of HOXC13-AS was lower in CC cells than normal cells (Figure 4A). A previous study reported that FTO, the m6A eraser, was up-regulated in CC and reduced m6A level of β-catenin mRNA in CC cells to induce its stability [33]. Therefore, we speculated that FTO was responsible for HOXC13-AS up-regulation. Concordantly, we confirmed FTO up-regulation in CC specimens and its positive correlation with HOXC13-AS (Figure 4B). Up-regulation of FTO in CC cell lines was verified (Figure 4C). Silencing FTO reduced FTO and HOXC13-AS expressions in CC cells (Figure 4D). The m6A level on HOXC13-AS increased upon FTO depletion (Figure 4E). After ActD treatment, the half-life of HOXC13-AS was shortened by FTO silence (Figure 4F). These data suggested that FTO stabilized and up-regulated HOXC13-AS by reducing m6A.

Finally, we looked whether FZD6 was required for the modulatory function of HOXC13-AS in CC. We confirmed that pcDNA3.1/FZD6 restored mRNA and protein of FZD6 reduced by sh-HOXC13-AS#1 (Figure 4G). FZD6 overexpression recovered the

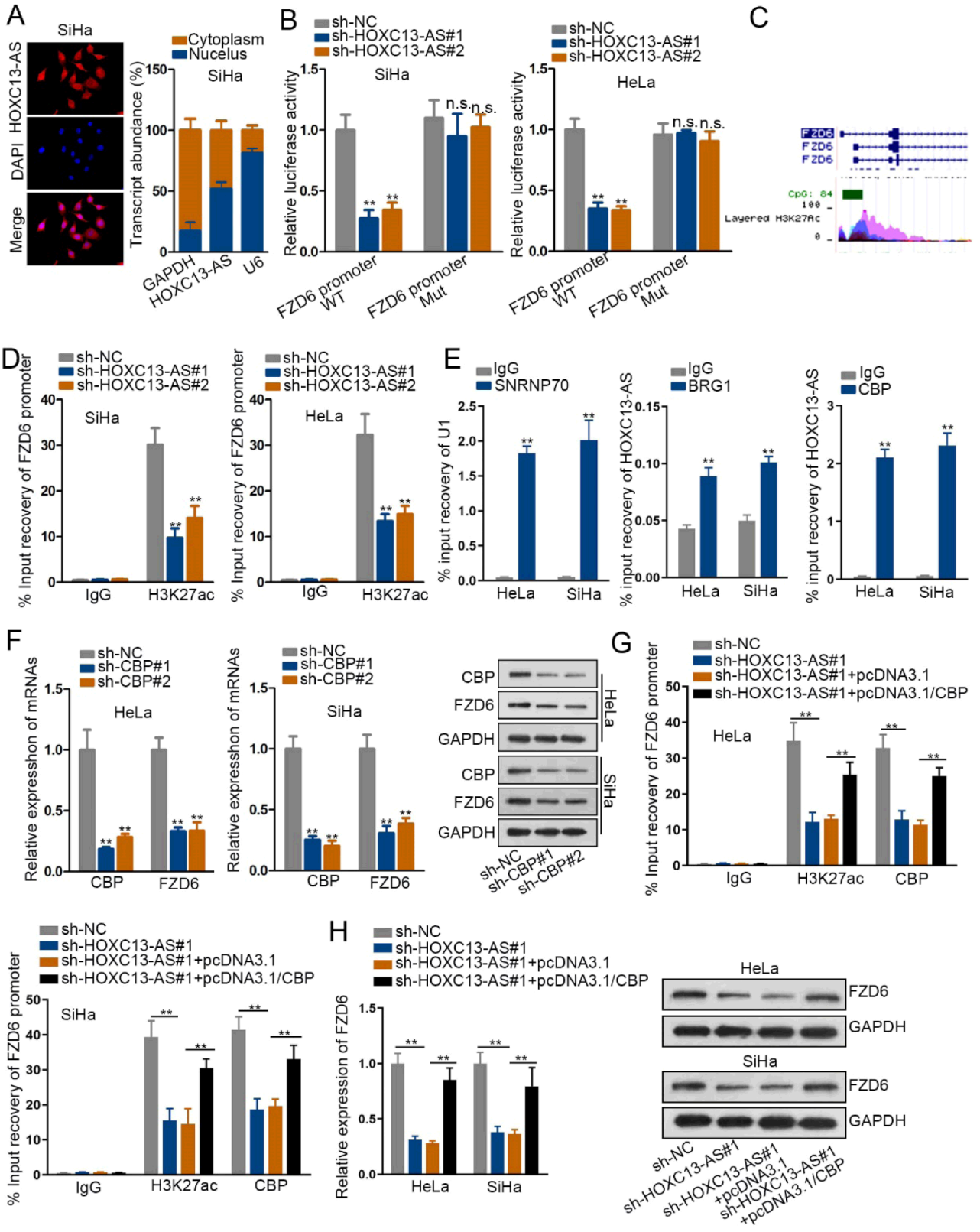

Figure 3. HOXC13-AS induced H3K27ac on FZD6 promoter through interacting with CBP. **A:** FISH and subcellular fractionation for HOXC13-AS in CC cells. **B:** Luciferase activity of FZD6 promoter WT/Mut after silencing HOXC13-AS. **C:** UCSC data for H3K27ac enrichment at CpG island of FZD6 promoter. **D:** ChIP analysis of FZD6 promoter in H3K27ac precipitates after HOXC13-AS depletion. **E:** RIP assay for HOXC13-AS enrichment in BRG1 or CBP-binding complex. **F:** RT-qPCR data and western blots CBP and FZD6 levels responding to CBP knockdown. **G:** ChIP analysis for the enrichment of H3K27ac and CBP on FZD6 promoter in CC cells transfected with sh-NC, sh-HOXC13-AS#1 or sh-HOXC13-AS#1+pcDNA3.1/CBP, sh-HOXC13-AS1#1+pcDNA 3.1. **H:** RT-qPCR and western blotting for FZD6 expression in each group. **p<0.01.

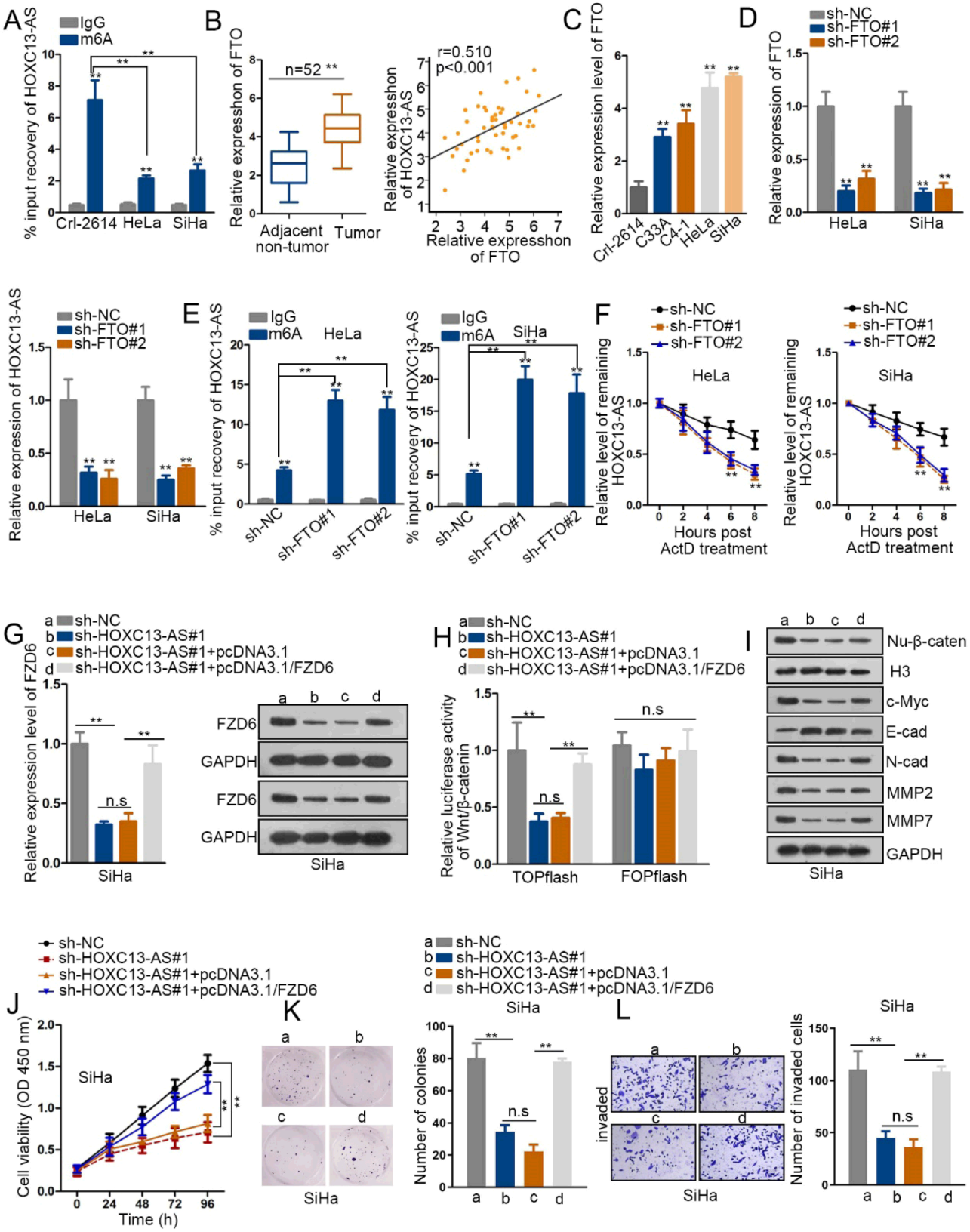

Figure 4. FTO-stabilized HOXC13-AS facilitated CC cell proliferation, invasion and Wnt/β-catenin activity through FZD6. **A:** The m6A level in Crl-2614, SiHa and HeLa cell lines was detected by m6A RIP. **B:** FTO up-regulation in CC tissues and its positive correlation with HOXC13-AS. **C:** FTO level in CC cell lines versus normal cells according to qRT-PCR. **D:** qRT-PCR testified silencing FTO on FTO and HOXC13-AS levels. **E:** The m6A level on HOXC13-AS upon FTO depletion. **F:** qRT-PCR analysis of remaining HOXC13-AS after ActD treatment upon FTO silence. **G:** SiHa cells were treated with sh-NC, sh-HOXC13-AS#1, sh-HOXC13-AS#1+pcDNA3.1 or sh-HOXC13-AS#1+pcDNA3.1/FZD6. RT-qPCR and western blots of FZD6. **H-I:** TOP/FOP-flash activity of Wnt/β-catenin and western blots of downstream effectors were examined in each group. **J-L:** Proliferation and invasion of SiHa of indicated each group. **p<0.01.

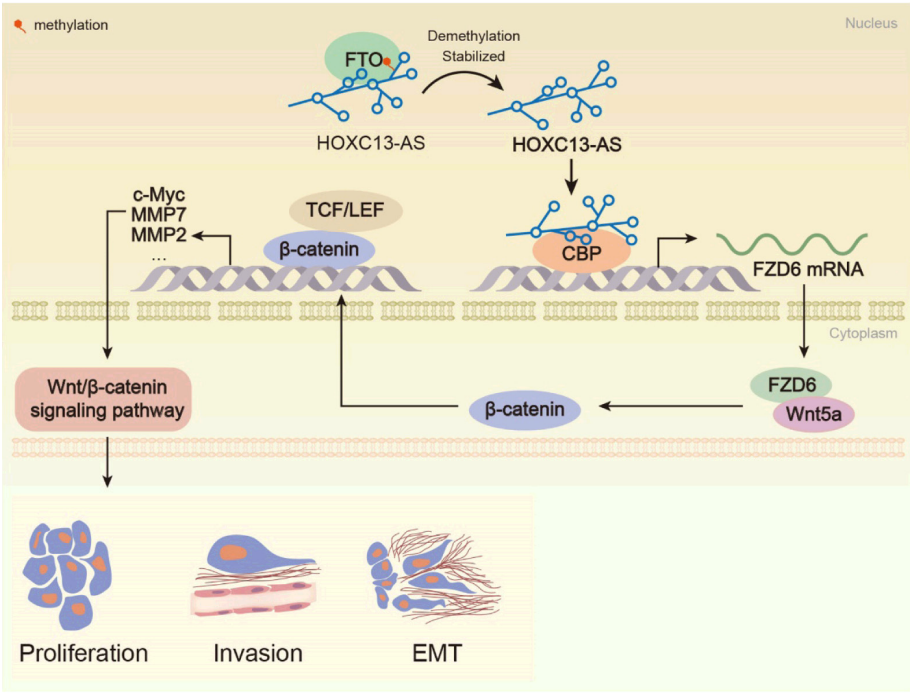

Figure 5. Graphical abstract. FTO-stabilized lncRNA HOXC13-AS epigenetically up-regulated FZD6 and activated Wnt/β-catenin signaling to drive cervical cancer proliferation, invasion and EMT.

activity of Wnt/β-catenin and downstream effectors inhibited by HOXC13-AS (Figure 4H-4I). Proliferation and invasion as well as migration reduced by sh-HOXC13-AS1#1 were recovered by pcDNA3.1/FZD6 (Figure 4J-4L & Supplementary Figure 2A-2H). Then, we assumed whether FTO could regulate the expression of FZD6 and Wnt/β-catenin signaling. Data of RT-qPCR and TOP/FOP-flash luciferase report assays revealed that FZD6 expression and the activity of Wnt/β-catenin were reduced by FTO down-regulation (Supplementary Figure 2I-2J).

Discussion

FZD6 is demonstrated as either activator or suppressor of Wnt/β-catenin pathway [12-14]. A previous study suggested that the function of FZD6 on canonical Wnt signaling may depend on cell type [14]. Hence, we were prompted to investigate how FZD6 functioned in CC. TCGA data and RT-qPCR analysis showed the up-regulation of FZD6 in CC, indicating its participation in CC. Functionally, FZD6 knockdown reduced proliferation, invasion and Wnt/β-catenin activity in CC cells, indicating that FZD6 served as an oncogene via positively affecting Wnt/β-catenin in CC.

LncRNAs are increasingly becoming a research hot-spot in cancer progression for their multilevel regulation on gene expression and potential to be therapeutic targets in cancers [19,20]. Previous studies showed that HOXC13-AS exerted carcinogenic functions in breast and nasopharyngeal cancers [22,23]. Herein, we firstly revealed that HOXC13-AS was up-regulated and positively related to FZD6 in CC according to TCGA and RT-qPCR data, indicating it as a potent regulator of FZD6. Mechanistically, we demonstrated that FZD6 was induced by H3K27ac, a kind of histone post-translational modification [35]. Previous studies showed that lncFZD6 induced H3K27ac on FZD6 through BRG1 [14]. However, we found that HOXC13-AS could not interact with BRG1. Instead, we firstly identified the interaction between CBP and HOXC13-AS. CBP is a histone acetyltransferase (HAT) which works with its highly homologous paralog EP300 to regulate chromatin remodeling and activate certain oncogenes in cancers [36-38]. Our study firstly showed that HOXC13-AS interacted with CBP to induce H3K27ac on FZD6.

Moreover, we showed that HOSX13-AS was stabilized by FTO, an m6A eraser in CC. The m6A modification is reported to improve or abrogate mRNA stability [26,27]. Formerly, a study showed that lncRNA RP11 was stabilized by inducing m6A level [28]. However, another study showed that FTO, the m6A eraser, was up-regulated in CC and reduced m6A level of CTNNB1 to stabilize its mRNA [33]. We firstly revealed that m6A level of HOXC13-AS was reduced in CC cells and that FTO reduced m6A on HOXC13-AS to improve its stability.

Conclusions

In conclusion, our study firstly illustrated that FTO-stabilized lncRNA HOXC13-AS epigenetically up-regulated FZD6 and activated Wnt/β-catenin signaling to drive cervical cancer proliferation, invasion, and EMT (Figure 5), indicating that FZD6 acted as an oncogene in CC and suggesting HOXC13-AS as a novel potential target for CC treatment.

Acknowledgement

Thanks a lot to all individuals or teams that were involved in our research.

Conflict of interests

The authors declare no conflict of interests.

References

1. Chen W, Zheng R, Baade PD et al. Cancer statistics in China, 2015. CA Cancer J Clin 2016;66:115-32.
2. Robbins AS, Han X, Ward EM, Simard EP, Zheng Z, Jemal A. Association Between the Affordable Care Act Dependent Coverage Expansion and Cervical Cancer Stage and Treatment in Young Women. JAMA 2015;314:2189-91.
3. Griess B, Tom E, Domann F, Teoh-Fitzgerald M. Extracellular superoxide dismutase and its role in cancer. Free Radic Biol Med 2017;112:464-79.
4. MacDonald BT, He X. Frizzled and LRP5/6 receptors for Wnt/beta-catenin signaling. Cold Spring Harb Perspect Biol 2012;4
5. Ruenraroengsak P, Kiryushko D, Theodorou IG et al. Frizzled-7-targeted delivery of zinc oxide nanoparticles to drug-resistant breast cancer cells. Nanoscale 2019;11:12858-70.
6. Kandyba E, Leung Y, Chen YB, Widelitz R, Chuong CM, Kobielak K. Competitive balance of intrabulge BMP/Wnt signaling reveals a robust gene network ruling stem cell homeostasis and cyclic activation. Proc Natl Acad Sci U S A 2013;110:1351-6.
7. Bengochea A, de Souza MM, Lefrancois L et al. Common dysregulation of Wnt/Frizzled receptor elements in human hepatocellular carcinoma. Br J Cancer 2008;99:143-50.
8. Wu QL, Zierold C, Ranheim EA. Dysregulation of Frizzled 6 is a critical component of B-cell leukemogenesis in a mouse model of chronic lymphocytic leukemia. Blood 2009;113:3031-9.
9. Saramaki OR, Porkka KP, Vessella RL, Visakorpi T. Genetic aberrations in prostate cancer by microarray analysis. Int J Cancer 2006;119:1322-9.
10. Vincan E, Barker N. The upstream components of the Wnt signalling pathway in the dynamic EMT and MET associated with colorectal cancer progression. Clin Exp Metastasis 2008;25:657-63.
11. Corda G, Sala G, Lattanzio R et al. Functional and prognostic significance of the genomic amplification of frizzled 6 (FZD6) in breast cancer. J Pathol 2017;241:350-61.
12. Golan T, Yaniv A, Bafico A, Liu G, Gazit A. The human Frizzled 6 (HFz6) acts as a negative regulator of the canonical Wnt. beta-catenin signaling cascade. J Biol Chem 2004;279:14879-88.
13. Lyons JP, Mueller UW, Ji H et al. Wnt-4 activates the canonical beta-catenin-mediated Wnt pathway and binds Frizzled-6 CRD: functional implications of Wnt/beta-catenin activity in kidney epithelial cells. Exp Cell Res 2004;298:369-87.
14. Deng J, Wang P, Chen X et al. FUS interacts with ATP synthase beta subunit and induces mitochondrial unfolded protein response in cellular and animal models. Proc Natl Acad Sci U S A 2018;115:E9678-86.
15. Jiang S, Kong P, Liu X, Yuan C, Peng K, Liang Y. LncRNA FLVCR1-AS1 accelerates osteosarcoma cells to proliferate, migrate and invade via activating wnt/beta-catenin pathway. JBUON 2020;25:2078-85.
16. Yan J, Wang R, Wu Z. LncRNA TCONS_l2_00002973 correlates with less advanced tumor stage and favorable survival, and also inhibits cancer cells proliferation while enhancing apoptosis in triple-negative breast cancer. JBUON 2019;24:535-42.
17. Fu X, Zhang L, Dan L, Wang K, Xu Y. LncRNA EWSAT1 promotes ovarian cancer progression through targeting miR-330-5p expression. Am J Transl Res 2017;9:4094-103.
18. Zhuang H, Cao G, Kou C, Li D. Overexpressed lncRNA CDKN2B-AS1 is an independent prognostic factor for liver cancer and promotes its proliferation. JBUON 2019;24:1441-8.
19. Chen F, Qi S, Zhang X, Wu J, Yang X, Wang R. lncRNA PLAC2 activated by H3K27 acetylation promotes cell proliferation and invasion via the activation of Wnt/betacatenin pathway in oral squamous cell carcinoma. Int J Oncol 2019;54:1183-94.
20. Zhang G, Cai J. Evaluation of prognostic value of lncRNA BANCR in tumor patients: A systematic review and meta-analysis. JBUON 2019;24:2553-9.
21. Han D, Wang J, Cheng G. LncRNA NEAT1 enhances the radio-resistance of cervical cancer via miR-193b-3p/CCND1 axis. Oncotarget 2018;9:2395-409.
22. Li X, Wang Q, Rui Y et al. HOXC13-AS promotes breast cancer cell growth through regulating miR-497-5p/PTEN axis. J Cell Physiol 2019;234:22343-51.
23. Gao C, Lu W, Lou W, Wang L, Xu Q. Long noncoding RNA HOXC13-AS positively affects cell proliferation and invasion in nasopharyngeal carcinoma via modulating miR-383-3p/HMGA2 axis. J Cell Physiol 2019;234:12809-20.

24. Desrosiers R, Friderici K, Rottman F. Identification of methylated nucleosides in messenger RNA from Novikoff hepatoma cells. Proc Natl Acad Sci U S A 1974;71:3971-5.
25. Fu Y, Dominissini D, Rechavi G, He C. Gene expression regulation mediated through reversible m(6)A RNA methylation. Nat Rev Genet 2014;15:293-306.
26. Pan T. N6-methyl-adenosine modification in messenger and long non-coding RNA. Trends Biochem Sci 2013;38:204-9.
27. Niu Y, Zhao X, Wu YS, Li MM, Wang XJ, Yang YG. N6-methyl-adenosine (m6A) in RNA: an old modification with a novel epigenetic function. Genomics Proteomics Bioinformatics 2013;11:8-17.
28. Wu Y, Yang X, Chen Z et al. m(6)A-induced lncRNA RP11 triggers the dissemination of colorectal cancer cells via upregulation of Zeb1. Mol Cancer 2019;18:87.
29. Coker H, Wei G, Brockdorff N. m6A modification of non-coding RNA and the control of mammalian gene expression. Biochim Biophys Acta Gene Regul Mech 2019;1862:310-8.
30. Lin Y, Ueda J, Yagyu K et al. Association between variations in the fat mass and obesity-associated gene and pancreatic cancer risk: a case-control study in Japan. BMC Cancer 2013;13:337.
31. Tan A, Dang Y, Chen G, Mo Z. Overexpression of the fat mass and obesity associated gene (FTO) in breast cancer and its clinical implications. Int J Clin Exp Pathol 2015;8:13405-10.
32. Zhu Y, Shen J, Gao L, Feng Y. Estrogen promotes fat mass and obesity-associated protein nuclear localization and enhances endometrial cancer cell proliferation via the mTOR signaling pathway. Oncol Rep 2016;35:2391-7.
33. Zhou S, Bai ZL, Xia D et al. FTO regulates the chemoradiotherapy resistance of cervical squamous cell carcinoma (CSCC) by targeting beta-catenin through mRNA demethylation. Mol Carcinog 2018;57:590-7.
34. Bose DA, Donahue G, Reinberg D, Shiekhattar R, Bonasio R, Berger SL. RNA Binding to CBP Stimulates Histone Acetylation and Transcription. Cell 2017;168:135-49.
35. Wang S, Zang C, Xiao T et al. Modeling cis-regulation with a compendium of genome-wide histone H3K27ac profiles. Genome Res 2016;26:1417-29.
36. Saha RN, Pahan K. HATs and HDACs in neurodegeneration: a tale of disconcerted acetylation homeostasis. Cell Death Differ 2006;13:539-50.
37. Marks P, Rifkind RA, Richon VM, Breslow R, Miller T, Kelly WK. Histone deacetylases and cancer: causes and therapies. Nat Rev Cancer 2001;1:194-202.
38. Khan O, La Thangue NB. HDAC inhibitors in cancer biology: emerging mechanisms and clinical applications. Immunol Cell Biol 2012;90:85-94.

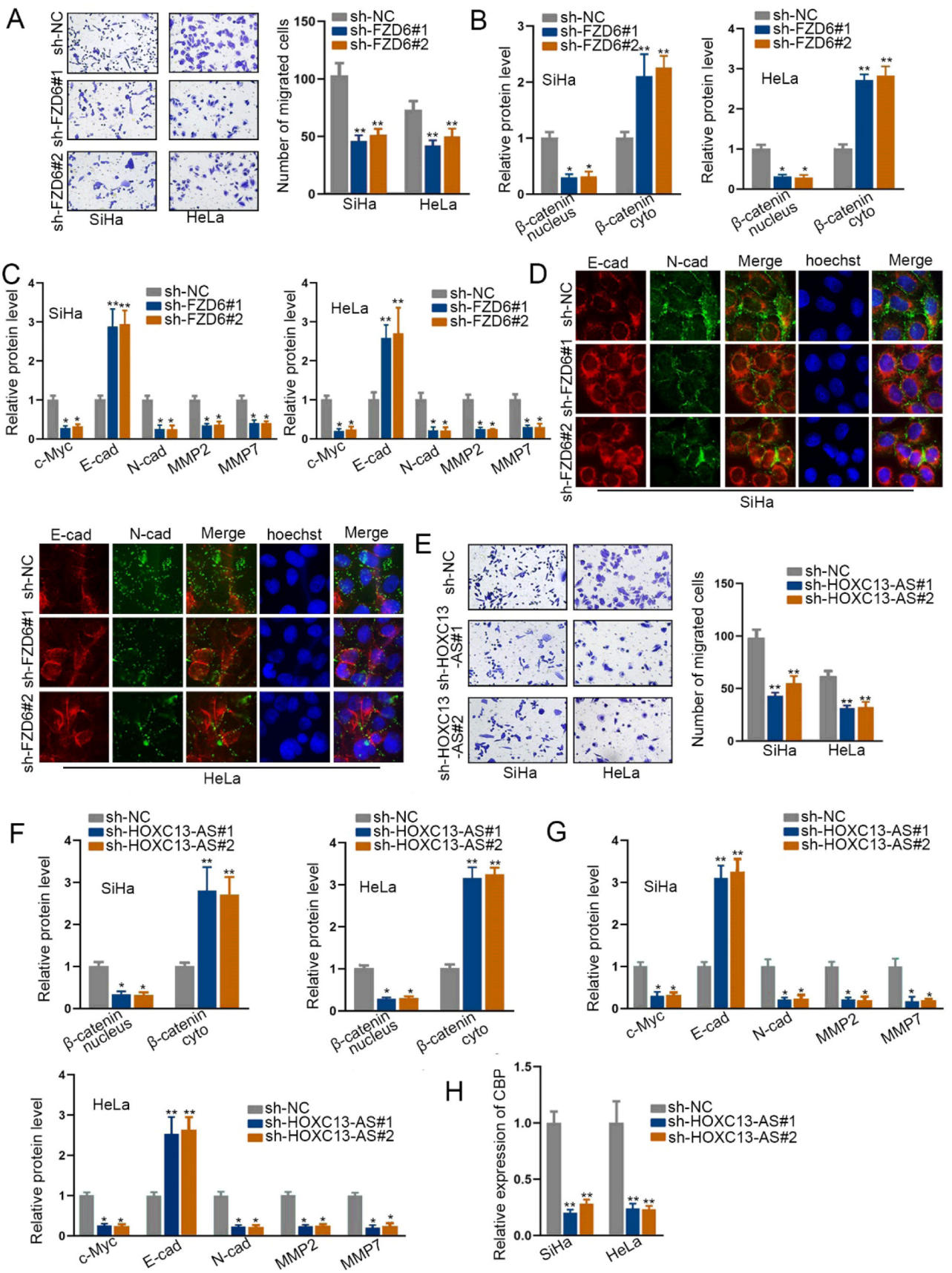

Supplementary Figure 1. A: Transwell assays were constructed to assess migratory capacities in cells transfected with sh-FZD6#1/2. **B-C:** Quantification of western blotting images was shown. **D:** Immunofluorescence of EMT process of CC cells after FZD6 knockdown. **E:** Transwell assays were performed to evaluate migration in cells transfected with sh-HOXC13-AS1#1/2. **F-G:** Quantification of western blotting images was shown. **H:** RT-qPCR was set up to measure CBP expression in cells transfected with sh-HOXC13-AS#1/2. *p<0.05; **p<0.01.

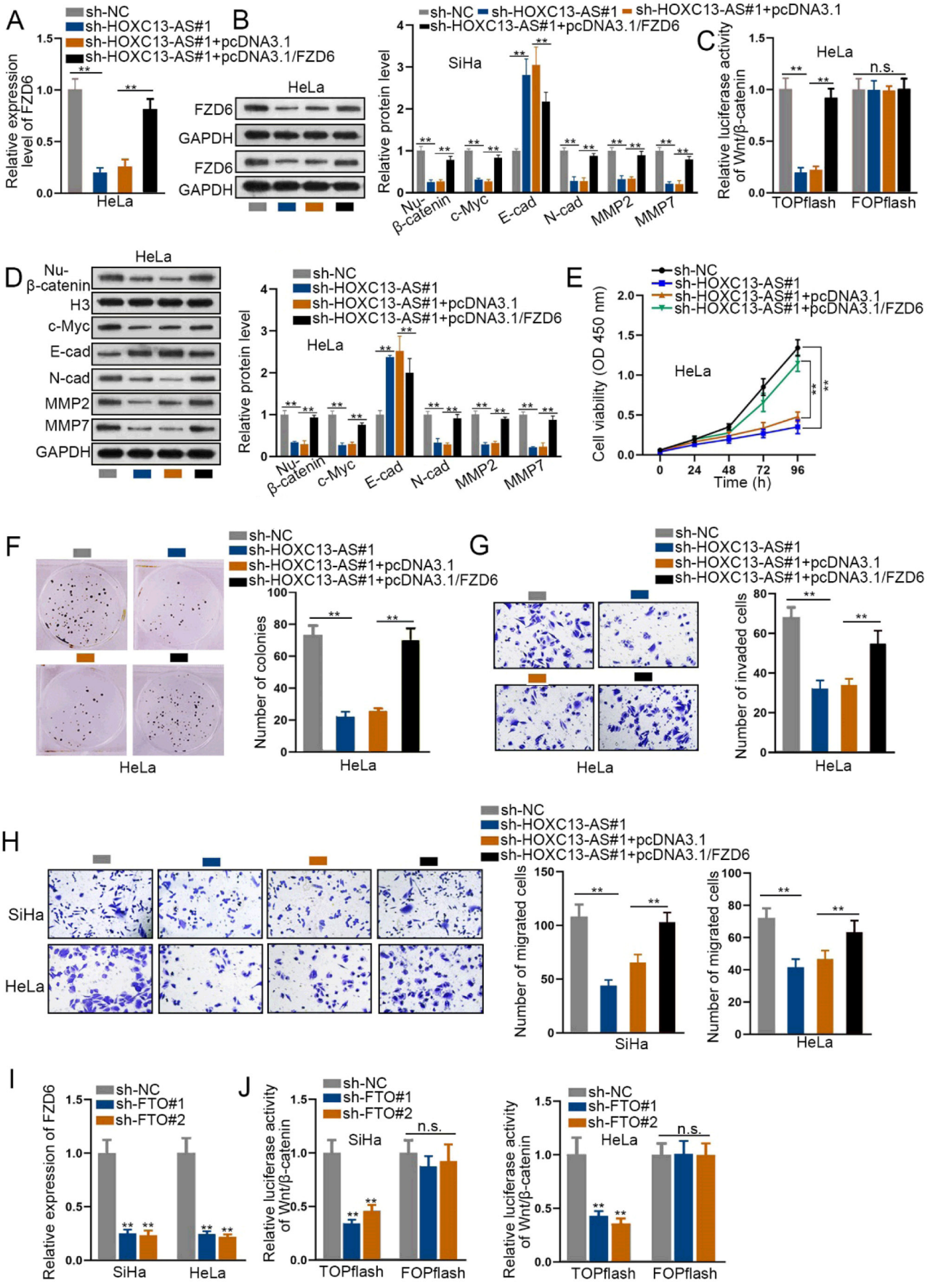

Supplementary Figure 2. A-H: Additional rescue assays in HeLa cell were assessed. **I:** FZD6 expression was examined in cells transfected with sh-FTO#1/2 by RT-qPCR. **J:** TOP-FOP flash analysis of Wnt/β-catenin activity under FTO silence. **p<0.01.